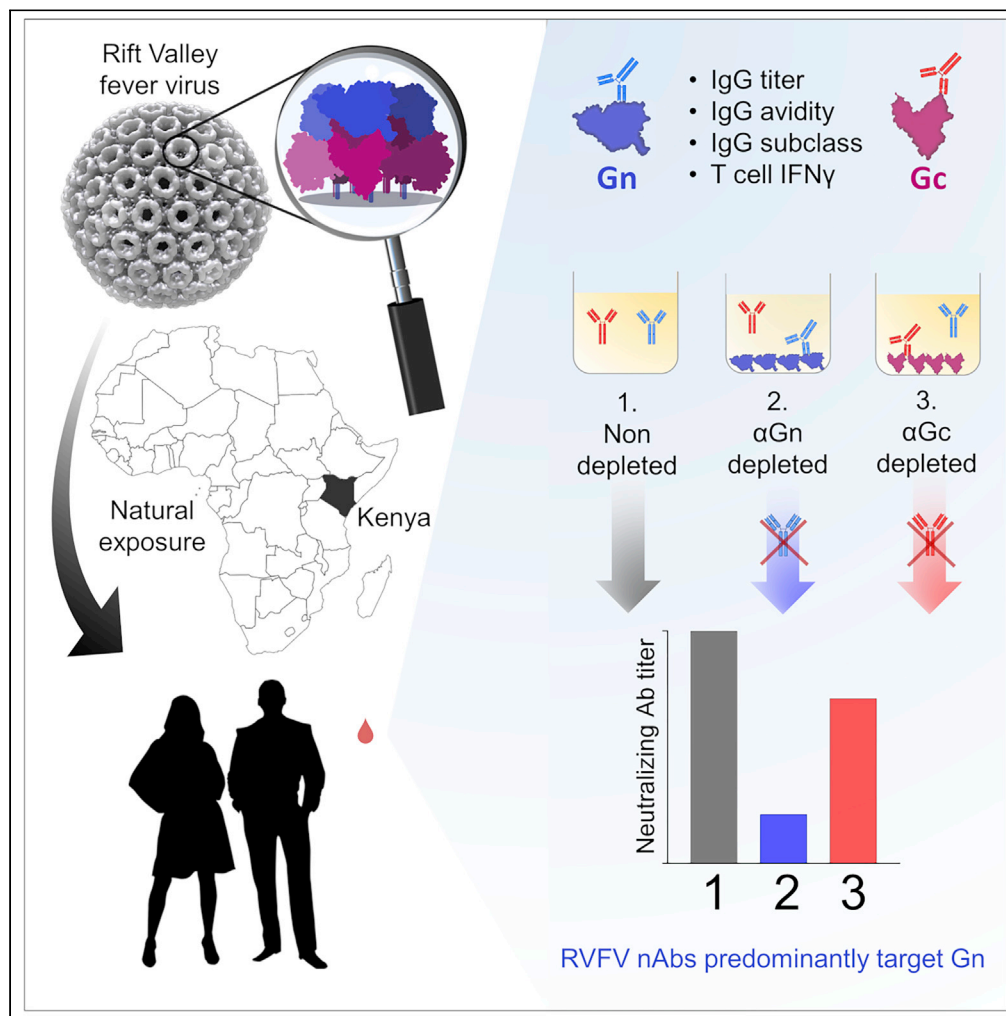## Article

Naturally Acquired Rift Valley Fever Virus Neutralizing Antibodies Predominantly Target the Gn Glycoprotein

Daniel Wright, Elizabeth R. Allen, Madeleine H.A. Clark, ..., Bernard Bett, Thomas A. Bowden, George M. Warimwe

danny.wright@ndm.ox.ac.uk

HIGHLIGHTS

Long-lasting antibodies, predominantly IgG1, target both RVFV glycoproteins

Gn is the principle target of the long-lived RVFV-neutralizing antibody response

IFNγ production from Gn/Gc-specific T cells is modest

iScience

Article

Naturally Acquired Rift Valley Fever Virus Neutralizing Antibodies Predominantly Target the Gn Glycoprotein

Daniel Wright,[1,2,7,*] Elizabeth R. Allen,[3] Madeleine H.A. Clark,[4] John N. Gitonga,[1] Henry K. Karanja,[1] Ruben J.G. Hulswit,[3] Iona Taylor,[2] Sumi Biswas,[2] Jennifer Marshall,[2] Damaris Mwololo,[5] John Muriuki,[5] Bernard Bett,[5] Thomas A. Bowden,[3] and George M. Warimwe[1,6]

SUMMARY

Rift Valley fever (RVF) is a viral hemorrhagic disease first discovered in Kenya in 1930. Numerous animal studies have demonstrated that protective immunity is acquired following RVF virus (RVFV) infection and that this correlates with acquisition of virus-neutralizing antibodies (nAbs) that target the viral envelope glycoproteins. However, naturally acquired immunity to RVF in humans is poorly described. Here, we characterized the immune response to the viral envelope glycoproteins, Gn and Gc, in RVFV-exposed Kenyan adults. Long-lived IgG (dominated by IgG1 subclass) and T cell responses were detected against both Gn and Gc. However, antigen-specific antibody depletion experiments showed that Gn-specific antibodies dominate the RVFV nAb response. IgG avidity against Gn, but not Gc, correlated with nAb titers. These data are consistent with the greater level of immune accessibility of Gn on the viral envelope surface and confirm the importance of Gn as an integral component for RVF vaccine development.

INTRODUCTION

Rift Valley fever (RVF) is one of several epidemic diseases prioritized by the World Health Organization and other global organizations for urgent research and development of control interventions (Mehand et al., 2018; Gouglas et al., 2018). The disease was first described in Kenya in 1930, but RVF epidemics are now commonly reported in Africa and the Arabian Peninsula (CDC, 2020). RVF is caused by the mosquito-borne Rift Valley fever virus (RVFV), a single-stranded RNA *Phlebovirus* in the *Phenuiviridae* family (ICTV, 2020). The virus primarily infects ruminants resulting in high rates of neonatal mortality and abortion that translate to major economic losses in the livestock industry of affected countries. Zoonotic transmission to humans most commonly occurs during livestock epizootics through infectious mosquito bites or direct contact with tissue or fluid from infected animals (Daubney et al., 1931; Nicholas et al., 2014). A wide spectrum of clinical manifestations characterize RVF in humans, including self-limiting mild illness associated with fever, myalgia, and other non-specific symptoms, through to hemorrhagic and neurological manifestations with high case fatality and debilitating sequela (reviewed in Wright et al., 2019) and possible miscarriage in pregnant women (Baudin et al., 2016; Adam and Karsany, 2008; Arishi et al., 2006). No therapeutics or vaccines are currently approved for human use, although several candidate vaccines are in development (Gouglas et al., 2018).

RVFV contains a tripartite genome consisting of a small (S), medium (M), and large (L) segment (Wright et al., 2019). The S segment encodes the nucleoprotein (N) and a non-structural protein (NSs). The L segment encodes the RNA-dependent RNA polymerase. The M segment encodes the structural glycoproteins, Gn and Gc. These two glycoproteins form heterodimers arranged into higher order pentamers and hexamers that encapsulate the mature virion and are responsible for host-cell attachment and membrane fusion (Halldorsson et al., 2018; Freiberg et al., 2008; Sherman et al., 2009; Huiskonen et al., 2009). They are the prime targets of neutralizing antibodies. Through the use of alternative translation sites and post-translational cleavage, the M segment also encodes for a non-structural protein (NSm) and a 78 kDa protein, which may play a structural role in virus derived from mosquito cells (Weingartl et al., 2014).

[1]KEMRI-Wellcome Trust Research Programme, CGMRC, PO Box 230-80108, Kilifi, Kenya

[2]The Jenner Institute, University of Oxford, Oxford OX3 7DQ, UK

[3]Wellcome Centre for Human Genetics, Division of Structural Biology, University of Oxford, Roosevelt Drive, Oxford OX3 7BN, UK

[4]London School of Hygiene & Tropical Medicine, London WC1E 7HT, UK

[5]International Livestock Research Institute, PO Box 30709, Nairobi 00100, Kenya

[6]Centre for Tropical Medicine and Global Health, University of Oxford, Oxford OX3 7FZ, UK

[7]Lead Contact

*Correspondence: danny.wright@ndm.ox.ac.uk

https://doi.org/10.1016/j.isci.2020.101669

Historical seminal studies in livestock and non-human primates demonstrated that immunity to RVF is acquired following recovery from RVFV infection and that this can be passively transferred to susceptible animals through administration of convalescent sera (Peters et al., 1988; Daubney et al., 1931). These studies identified viral neutralizing antibodies (nAbs), which target the RVFV Gn and Gc envelope glycoproteins, as the main correlates of protection against RVF (Easterday, 1965). Occupational exposure to RVFV infection during the decades following the discovery of RVFV provided the first evidence of naturally acquired RVFV nAbs and these tended to be long-lived, being readily detectable in two individuals 12 and 25 years post-infection, respectively, despite no further exposure (Smithburn et al., 1949; Brown et al., 1957; Findlay, 1936). However, beyond these studies, naturally acquired immunity to RVFV in humans is poorly described. Here, we sought to address this paucity of information by characterizing the humoral and cellular response to RVFV among naturally exposed adults in Kenya, including an investigation of the longevity and kinetics of RVFV nAbs in this population.

RESULTS

Stored samples from two adult populations in coastal Kenya were used for this study (see Methods). One population of adults comprised a random selection of fifty RVFV-exposed individuals included in a previous cross-sectional survey investigating the risk factors for RVFV exposure in Tana River county (Bett et al., 2018). The second population was composed of adults under longitudinal surveillance for malaria within the Kilifi Health and Demographic Surveillance System (KHDSS) (Scott et al., 2012) in Kilifi county and had previously not been screened for RVFV exposure (see Methods).

IgG Responses against Gn and Gc Correlate with RVFV nAb Levels

We first measured IgG antibody responses against Gn and Gc in fifty RVFV-exposed adults from Tana River county and assessed their relationship with the RVFV nAb response. The geometric mean titer (GMT) of RVFV nAb as measured by virus neutralizing assay (VNT_{50}) in these fifty adults was approximately 2,100 (95% confidence interval [CI] 1,543–2,792) and ranged between ~160 and >14,000 (Figure 1). Total IgG titers against Gn and Gc (ELISA GMT of 67.3 for Gn and 66.9 for Gc) were highly correlated ($r = 0.77$, $p < 0.001$). A strong correlation was observed between the RVFV nAb titer and IgG response against Gn ($r = 0.76$, $p < 0.0001$) and Gc ($r = 0.68$, $p < 0.0001$) (Figure 1A). IgG1 subclass predominated the antibody response against both Gn and Gc (Figure 1C).

We also measured the avidity of the antibody response to each glycoprotein, expressing this as the concentration of NaSCN, a chaotropic agent, required to reduce ELISA signal by 50% (NaSCN IC_{50}). Anti-Gc antibody avidity was significantly higher than that for anti-Gn antibodies (Figure 1B); however, a correlation between antibody avidity and nAb response was only observed for Gn ($r = 0.37$, $p = 0.009$) and not Gc ($r = 0.08$, $p = 0.57$).

nAbs from Naturally Exposed Adults Preferentially Target RVFV Gn over Gc

We next investigated the relative contribution of Gn and Gc to the RVFV nAb response. To do this, we pooled available sera from seven RVFV-exposed adults from Tana River county who had high titers (>300 anti-Gn and anti-Gc AU). We then depleted the pooled serum of antibodies specific for one or both of the recombinant RVFV glycoproteins (see Methods). ELISA was used to confirm the depletion, showing a reduction in IgG endpoint titer of 98% and 93% for Gn and Gc, respectively, compared with non-depleted serum (Figure 2A). The impact of this antigen-specific antibody depletion on the ability of the pooled serum to neutralize RVFV *in vitro* was then measured by VNT_{50}. Anti-Gn antibody depletion resulted in a 79% reduction in nAb titer compared with the non-depleted serum (Figure 2B). In contrast, depletion of anti-Gc antibodies from sera showed a modest 29% reduction compared with the non-depleted serum (Figure 2B). Depletion of both Gn and Gc antibodies showed a 79% reduction in nAb titer, identical to the pool depleted of anti-Gn antibodies alone (Figure 2B).

Of 200 adults under longitudinal surveillance for malaria studies in Kilifi county, 6 (3%) in 2018 had evidence of RVFV exposure on the basis of carriage of RVFV nAbs (see Methods). To confirm the predominance of Gn as a target of the RVFV nAb response, we pooled sera from these six individuals and repeated the depletion experiment described above using a different assay to measure RVFV nAbs, focus reduction neutralization assay ($FRNT_{50}$; see Methods). Results were consistent, showing a relative reduction in $FRNT_{50}$ of
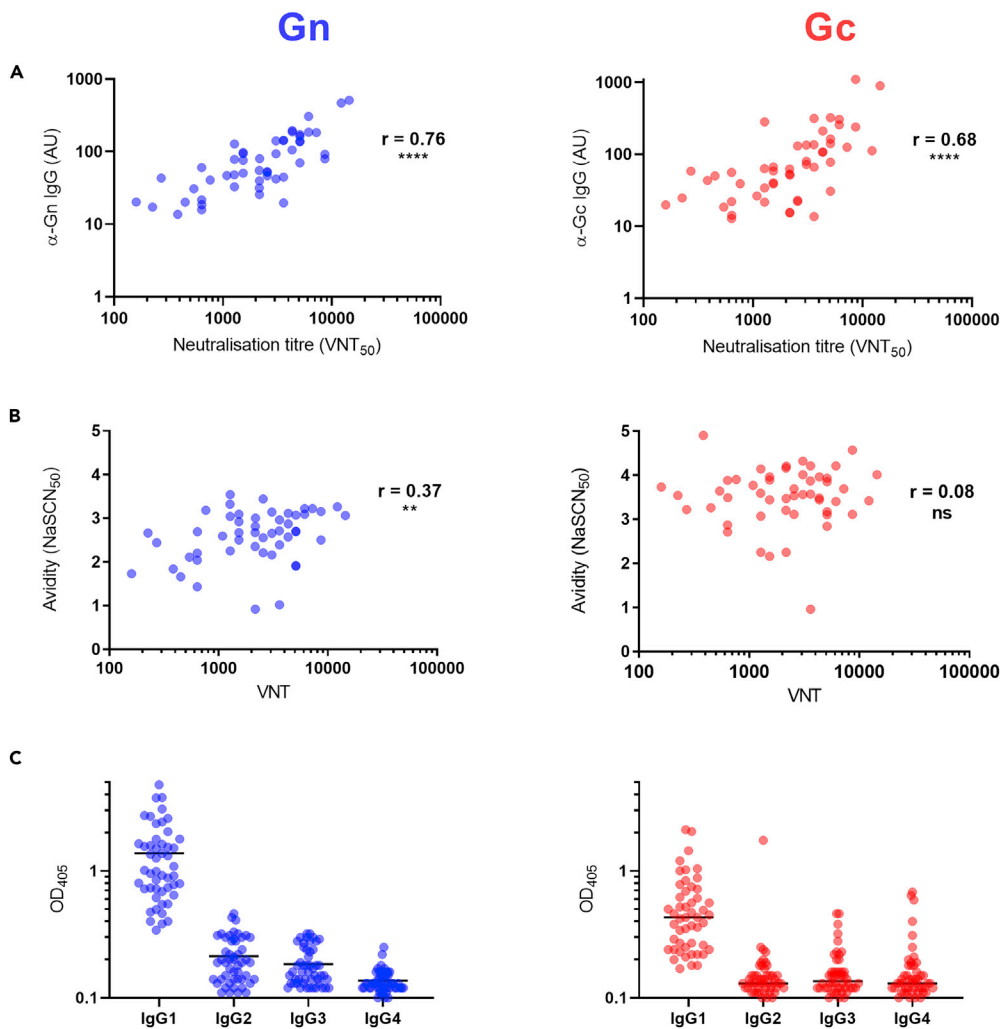
Figure 1. Total IgG Titer toward Recombinant Gn and Gc Correlate Strongly with Neutralizing Antibody Titer

(A) Correlations between neutralization titer, as measured by VNT_{50} assay, and total IgG titer toward Gn and Gc, as measured by ELISA (Gn: r = 0.76, 95% CI: 0.60–0.86. Gc; r = 0.68, 95%CI: 0.49–0.81).****p < 0.0001, Spearman's correlation.

(B) Correlations between neutralization titer and avidity of total IgG toward Gn and Gc (Gn: r = 0.37, 95% CI: 0.09–0.59, **; Gc: r = 0.08, 95% CI: −0.21–0.36, p = 0.57).**p = 0.009, Spearman's correlation.

(C) IgG subclass response toward Gn and Gc. Lines represent geometric means.

See also Figure S1 for recombinant protein expression.

approximately 76%, 14%, and 70% in sera depleted of antibodies to Gn, Gc, or both, respectively (Figure 2C). These data support RVFV Gn as the major target of the nAb response arising during natural RVFV infection.

IgG and RVFV nAb Titers Remain High over Many Years

To study longevity of the observed immune responses we used three of the six RVFV-exposed adults from Kilifi county who had corresponding stored serum samples spanning multiple years between 1998 and 2018 (see Methods). We also included stored sera from an additional two RVFV-exposed adults identified from the same surveillance study in previous years. Overall, the period covered by each individual's samples ranged from 3 to 11 years, but dates of RVFV exposure were unknown (Figure 3). Both IgG (anti-Gn and anti-Gc) and RVFV nAb titers were readily detected over the period of follow-up (Figure 3). In keeping with the two seminal studies on the durability of RVFV nAb titers, the individual from whom we had the highest number of samples, JA0073 (n = 8), exhibited high nAb titers over an 11-year period (Figure 3A). RVFV
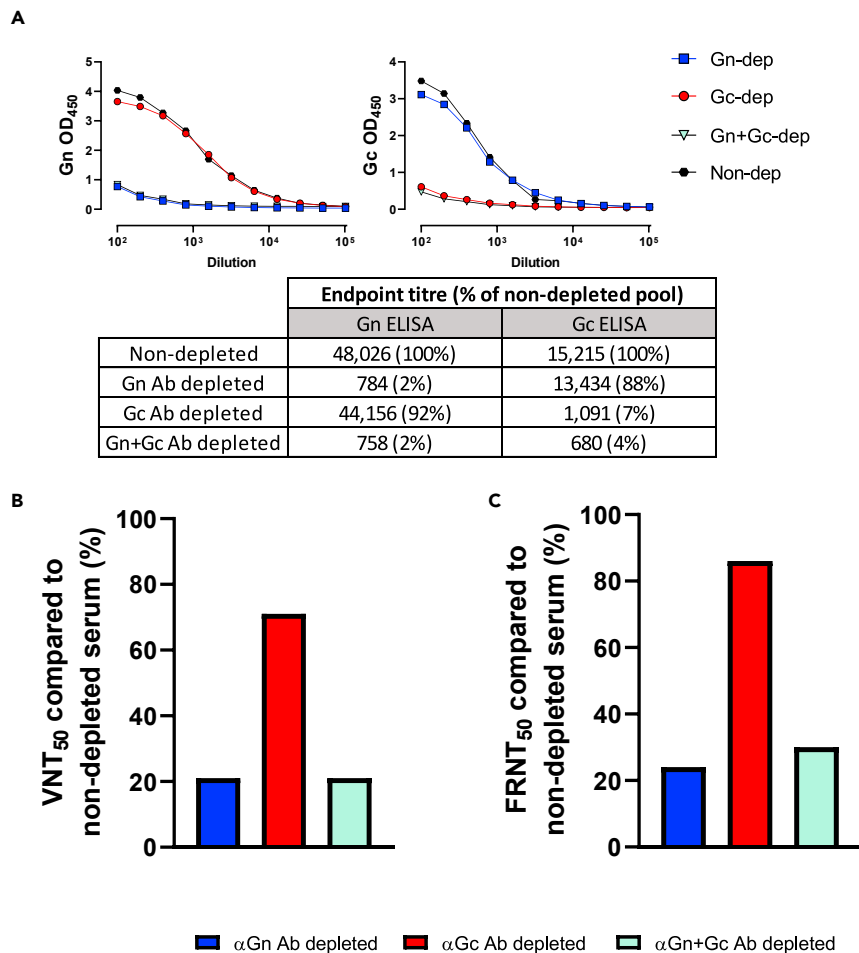
Figure 2. Neutralizing Antibody Titers Predominantly Target RVFV Gn over Gc

Individual sera were pooled from individuals in Tana River county (n = 7) and depleted of anti-Gn antibodies, anti-Gc antibodies, both, or neither.

(A) Confirmation of depletion by Gn ELISA (left) and Gc ELISA (right) with Gn and Gc Endpoint titers of each pool calculated in the table.

(B) Neutralization titer (VNT_{50}) of each depleted pool as a percentage of non-depleted serum (VNT_{50} of Gn antibody depletion, 1,600; Gc antibody depletion, 5,344; Gn + Gc antibody depletion, 1,600; non-depleted, 7,557).

(C) Neutralization titer ($FRNT_{50}$) after repeating experiment using an entirely different serum pooled from individuals from Kilifi county (n = 6) and confirming the same result.

nAb titers were generally stable with only slight reductions from individual peak nAb titers observed. Individual JA0073 was seronegative when sampled in 2007 but was strongly seropositive in 2008 suggesting they may have been exposed during 2007, when there was a major RVF epidemic in Kenya (Munyua et al., 2010). Individuals JA0176 and JA0193 had evidence of boosting of their nAb response (Figure 3), most likely as a result of interepidemic RVFV exposure as no RVF epidemics were reported in the country during their follow-up period. Total binding IgG titers toward both glycoproteins were also long-lasting, remaining high despite a gradual decline over the years, while avidity remained stable (Figures 3B and 3C).

RVFV Infection Elicits a Moderately Low but Significant Cellular Response to Gn and Gc

Cryopreserved PBMCs were also available from five of the RVFV-exposed adults sampled in 2018 from Kilifi county, allowing an assessment of RVFV-specific T cell responses. We measured Gn and Gc-specific IFNγ responses by ELISpot in five individuals and compared these with PBMCs from five randomly selected individuals from the same population who had no evidence of RVFV exposure (on the basis of lacking RVFV nAb or Gn/Gc IgG responses). Overall, the IFNγ response was moderately low in the five RVFV-exposed individuals (mean response 67.4 spot-forming cells (SFC)/10^6 PBMC 95% CI 6.8–128 SFC/10^6), but this
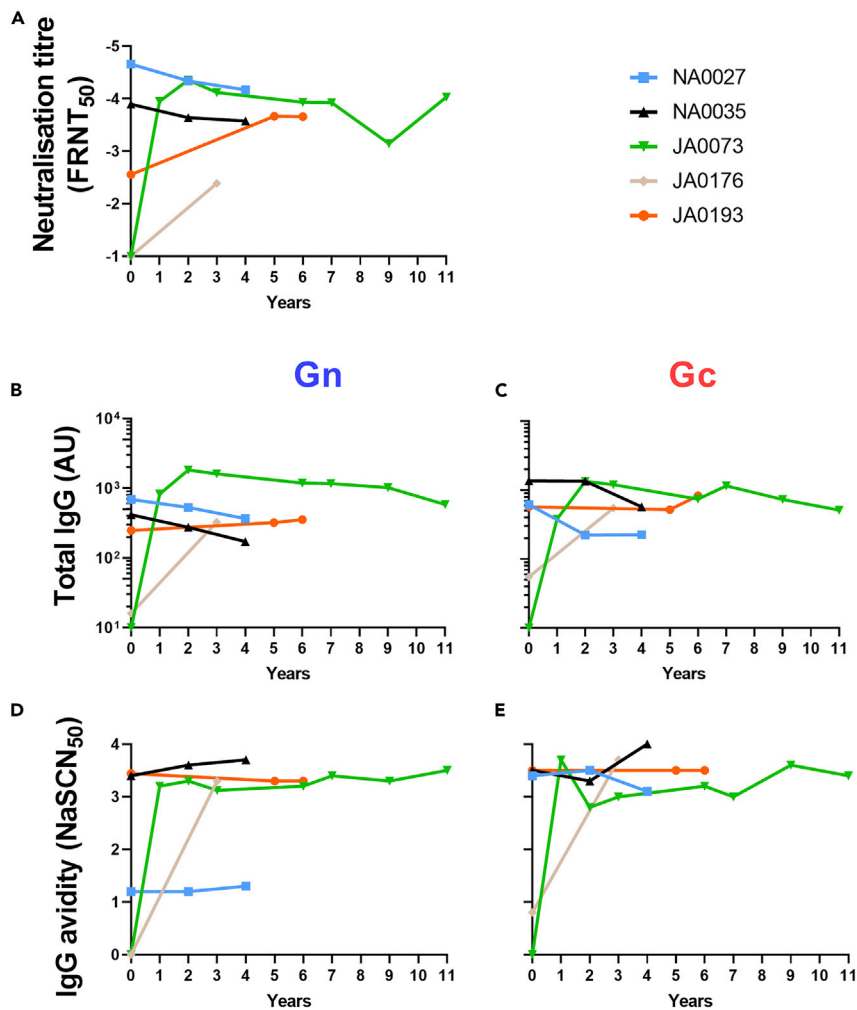
Figure 3. Natural Exposure to RVFV Elicits a High-Titer, Long-Lived Humoral Response

Five individuals from Kilifi county (see text) with serum samples spanning 3–11 years were assayed for (A) Neutralization titer, (B) Titer of anti-Gn IgG, (C), Titer of anti-Gc IgG , (D) Avidity of anti-Gn IgG, and (E) Avidity of anti-Gc IgG. Year 0 is their earliest available sample, not necessarily the year of exposure, with subsequent samples plotted relative to that. Individuals' serum samples were collected between the following years: NA0027 2014–2018; NA0035 2014–2018; JA0073 2007–2018; JA0176 2011–2014; JA0193 2007–2013.

was significantly higher than non-exposed controls (mean response 8.4 SFC/10^6 PBMC 95% CI 0–21.7 SFC/10^6) (Figure 4A). Responses among RVFV-exposed individuals were comparable across individual peptide pools (Figure 4B). Staphylococcal enterotoxin B (SEB) was used as a positive control for PBMC stimulation, and all unexposed and RVFV-exposed individuals had a response >1,900 SFC/10^6 PBMC as expected. Together, these data indicate that natural RVFV exposure elicits a durable T cell response.

DISCUSSION

The protective role antibodies play against RVFV infection is well documented (Peters et al., 1988; LaBeaud, 2010; Niklasson et al., 1984). The structural glycoproteins displayed on the surface of RVFV, Gn and Gc, are key targets of this protective immune response, and monoclonal antibodies have been identified targeting both (Besselaar and Blackburn, 1991; Besselaar-Blackburn, 1992; Wang et al., 2019). Studies of the live-attenuated MP-12 vaccine have shown neutralizing antibodies present in a majority of individuals at least 5 years post vaccination (Pittman et al., 2016). However, relatively little is known about the nature and longevity of the immune response after natural RVFV exposure. Here, using samples from adults in coastal Kenya with evidence of previous exposure to RVFV we show that: (1) RVFV Gn and Gc glycoproteins are
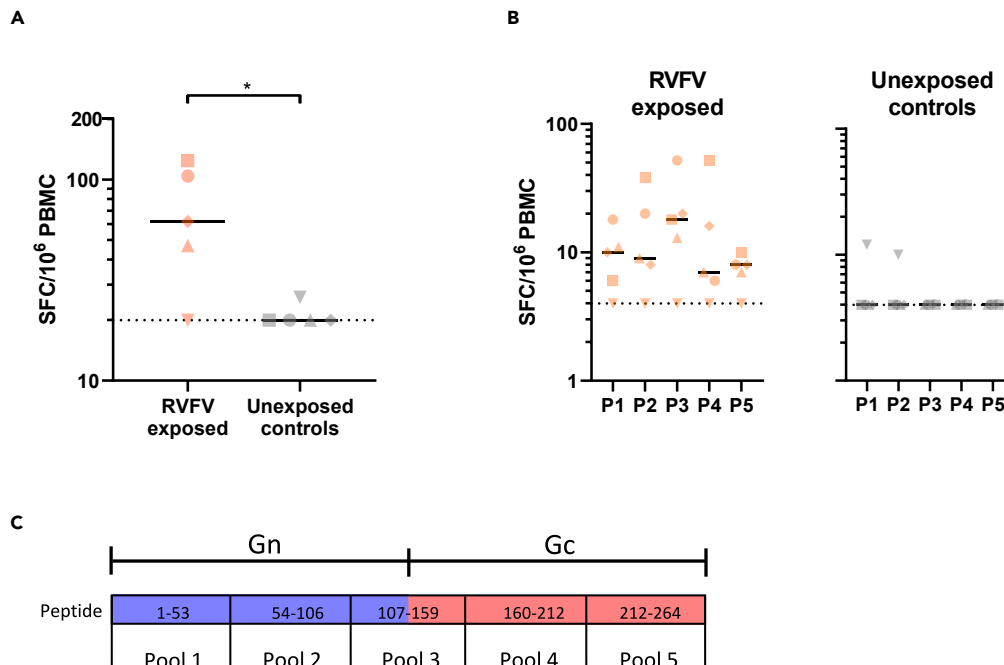
A

B

C

Figure 4. A Low but Significant *Ex Vivo* IFNγ ELISpot Response in Naturally Exposed Individuals

PBMC from five RVFV-exposed individuals along with five case-matched non-exposed controls were stimulated with an overlapping peptide library spanning the GnGc polyprotein.

(A) Summed responses from the five peptide pools showing significantly higher response in the naturally exposed group compared with naive controls (*$p < 0.05$, unpaired t test).

(B) Responses to individual peptide pools, dotted line represents the lower limit of detection of four spot-forming cells (SFC)/10^6 PBMC for individual pools and 20 SFC/10^6 PBMC for summed responses. SEB stimulated cells for each volunteer gave >1,900 SFC/10^6 PBMC.

(C) Schematic of the overlapping peptide library used for stimulation. Bars represent median.

both targets of the long-lived T cell and IgG response to RVFV and that the antibody response is predominated by the IgG1 sub-class, (2) RVFV nAb titers strongly correlate with Gn and Gc-specific IgG responses, and (3) Gn is the main target of the RVFV nAb response. We also found that IgG avidity against Gn (but not Gc) correlated with the RVFV nAb response, further highlighting qualitative differences in the antibody response to both glycoproteins.

Studies in mice and rabbits have identified monoclonal antibodies targeting either Gn or Gc that are able to neutralize virus and confer protection against RVFV challenge (Besselaar and Blackburn, 1991; Besselaar-Blackburn, 1992; Keegan and Collett, 1986; Allen et al., 2018; Wang et al., 2019). Initial hints of the possible greater role that antibodies targeting Gn play in protection, with respect to the Gc, came from reports suggesting passive transfer of anti-Gn and not anti-Gc antibodies was capable of providing protection in mice (Battles and Dalrymple, 1988). Another study in mice, this time involving vaccination with Gn- or Gc-coding DNA, showed that all those vaccinated with Gn seroconverted but only half of those vaccinated with Gc (Lagerqvist et al., 2009). A more recent study isolating mAbs from a convalescent human patient returning to China found that mAbs specific to Gn exhibited much higher neutralization titers than those that bind Gc (Wang et al., 2019). This provides some evidence, perhaps, that the larger negative impact on neutralization titer seen in our study after depleting antibodies targeting Gn, compared with Gc, reflects a greater neutralizing potential of anti-Gn antibodies rather than merely increased abundance over anti-Gc antibodies. Further evidence supporting this hypothesis can be observed from our measurement of IgG avidity. Higher avidity antibodies can bind antigen more efficiently, and only the higher avidity of anti-Gn antibodies was associated with increased nAb titer. Although avidity was very stable over many years, it is typically lower in acute or recent infection. However, owing to the sparse sampling (no more than once a year), initial changes in the weeks and months post exposure are not visible.

Our recombinantly derived RVFV Gn and Gc were secreted from HEK 293T cells and thus subject to the cellular folding checkpoints that exist in mammalian cells (Ellgaard and Helenius, 2003). Similar constructs and protein production methods have been used to successfully produce and crystallize phleboviral Gn (Halldorsson et al., 2018) and Gc glycoproteins (Halldorsson et al., 2016), as well as the Gn and Gc from related hantaviruses (Li et al., 2016; Rissanen et al., 2017; Rissanen et al., 2020), and their native-like fold architectures have been shown to be compatible with cryoEM-derived reconstructions of purified virions and virus-like particles (Halldorsson et al., 2018). These combined observations indicate that our recombinantly produced RVFV proteins can serve as "native-like" mimetics of RVFV Gn and Gc. However, it is also important to acknowledge that recombinant material will not completely match the native form of the virus. For example, the recombinant and putatively monomeric RVFV Gn and Gc used in these assays does not replicate their native higher-order, membrane-bound pentameric and hexameric Gn-Gc assemblies on the virion surface (Halldorsson et al., 2018). Although our data show that dual depletion of both Gn and Gc antibodies reduces nAb titers to identical levels seen in sera depleted of Gn antibodies alone, even dual-depleted sera can neutralize live virus at the highest concentration (Figure 2). Although this is likely due, at least in part, to the incomplete nature of the depletion (corresponding ELISA signal post depletion was not entirely eliminated at high serum concentrations), it is also likely that a subset of antibodies recognize epitopes constituting higher-order quaternary assemblies formed on the native virion surface. These antibodies may be capable of neutralizing whole virus but may not bind our recombinant Gn or Gc and therefore would not have been depleted. Nevertheless, we were still able to assess the relative contribution antibodies targeting each individual glycoprotein have on neutralization, demonstrating reproducibility of the effect in two different populations within Kenya, using two different measures of nAb. Although both glycoproteins are clearly immunogenic and targeted by the nAb response, our data suggest that after naturally acquired human infection antibodies targeting Gn, rather than Gc, play a larger role in RVFV neutralization. This is perhaps not surprising considering that the N-terminal component of Gn occupies the most membrane-distal region of the virus, which plays a role in shielding the cognate Gc (Halldorsson et al., 2018; Allen et al., 2018), and therefore may be more easily accessible to the host immune system (Figure S2).

Although protection against RVFV infection has long been associated with the induction of nAbs targeting Gn and Gc (Dodd et al., 2013; Peters et al., 1988; LaBeaud, 2010), it can also arise from other mechanisms. Mice vaccinated with the immunodominant nucleoprotein (N), for example, show partial protection from RVFV challenge despite the absence of detectable nAbs (Lopez-Gil et al., 2013; Jansen Van Vuren et al., 2011). Another study showed the cooperative effect of a non-neutralizing antibody improving protection in a mouse model (Gutjahr et al., 2020). Perhaps more surprisingly, mice vaccinated with modified Vaccinia Ankara (MVA) expressing both Gn and Gc failed to elicit nAbs but were still protected from viral challenge (Lopez-Gil et al., 2020). IgG1, the predominant subclass recognizing the RVFV glycoproteins identified here, can efficiently trigger the classical route of complement (Vidarsson et al., 2014). Although the contribution that non-neutralizing antibodies and cellular immunity have on protection against RVFV is less well characterized, numerous components of the immune response may function together during acute infection (including experimental challenge in animals) to provide protection. Studies on the immune response during acute RVFV infections in humans are needed to determine the role of other immune mechanisms in disease pathogenesis and protection.

Owing to its extensive anti-viral properties, we have used IFNγ as a broad measure of the cellular response to RVFV in these individuals. The *ex vivo* ELISpot carried out here is a measure of effector memory T cells that are able to secrete IFNγ within hours of re-exposure to antigen (Calarota and Baldanti, 2013). We have shown that these cells, circulating in the peripheral blood, are relatively low in number in humans with historical RVFV infection. However, they are still detectable in the majority of individuals many years after exposure and may potentially play an important role in protection. Recently, the T cell responses in human volunteers vaccinated with multiple doses of a formalin-inactivated RVF vaccine were characterized (Harmon et al., 2020). Despite also showing a generally low cellular response, IFNγ expression post stimulation with Gn, Gc, and N peptides were detected by ELISpot many years post vaccination. A previous study exploring the cellular response to RVFV in a non-human primate model has shown that non-lethal challenge was associated with early proliferation of CD4$^+$ and CD8$^+$ T cells in addition to early Th1 cytokine production, including IFNγ (Wonderlich et al., 2018). Another study in humans showed higher expression of IL-10, an anti-inflammatory cytokine, was associated with fatal cases (McElroy and Nichol, 2012). These findings, together with the critical role CD4+ T cells play in generating strong antibody responses (Dodd et al., 2013), indicate the importance and benefit of a robust cellular response.

Owing to the presence of high-titer, long-lived nAbs, it is plausible that the naturally acquired immune response to RVFV may be sufficient for long-lasting protection, particularly as nAbs are associated with protection in animals. The observation that antibodies targeting Gn play a comparatively larger role in neutralization than those that target Gc has potential implications for vaccine design and is suggestive that the Gn may be the most critical antigen to include in RVFV candidate vaccines.

We have provided data characterizing the immune response in a large number of naturally exposed Kenyan adults who are likely protected from re-exposure. These data can provide a useful benchmark for immune responses elicited in future clinical trials of candidate vaccines.

Limitations of the Study

Although our immunological assessments of individuals naturally exposed to RVFV provide useful data on immunity to infection, there is a lot that we do not know regarding their previous RVFV exposure. Precise dates on when the RVFV infections occurred were unknown, making it difficult to ascribe any acute febrile illnesses encountered by the individuals in the years preceding this study. Furthermore, given that RVFV can also cause self-limiting illness, active surveillance for the incidence of such infections would be the best approach to relate particular acute illnesses to a corresponding boost in immune responses. Additional unknowns include the route of exposure (mosquito bite versus contact with infected animal tissue), presence of co-infections, and their clinical manifestations. All of these factors will have likely influenced their subsequent response to RVFV and further work with larger sample sizes is needed to connect immunological attributes with clinical outcomes and disease severity.

Resource Availability

Lead Contact
Further information and requests for resources and reagents should be directed to and will be fulfilled by the Lead Contact, Daniel Wright (danny.wright@ndm.ox.ac.uk).

Materials Availability
Plasmids generated in this study are available from the Lead Contact with a completed Materials Transfer Agreement.

Data and Code Availability
The published article includes all datasets generated or analyzed during this study.

METHODS

All methods can be found in the accompanying Transparent Methods supplemental file.

SUPPLEMENTAL INFORMATION

Supplemental Information can be found online at https://doi.org/10.1016/j.isci.2020.101669.

AUTHOR CONTRIBUTIONS

Conceptualization, D.W., G.M.W., and T.A.B.; Methodology, D.W., E.R.A., J.N.G., H.K.K., and G.M.W.; Investigation, D.W., M.H.A.C., J.N.G., and H.K.K.; Resources, R.J.G.H., I.T., S.B., E.R.A., D.M., J.M., and B.B.; Writing – Original Draft, D.W.; Writing – Review & Editing, G.M.W. and T.A.B.; Funding acquisition, G.M.W. and T.A.B; Supervision; G.M.W. and T.A.B.

DECLARATION OF INTERESTS

The authors declare no competing interests.

REFERENCES

Adam, I., and Karsany, M.S. (2008). Case report: Rift Valley fever with vertical transmission in a pregnant Sudanese woman. J. Med. Virol. *80*, 929.

Allen, E.R., Krumm, S.A., Raghwani, J., Halldorsson, S., Elliott, A., Graham, V.A., Koudriakova, E., Harlos, K., Wright, D., Warimwe, G.M., et al. (2018). A protective monoclonal antibody targets a site of vulnerability on the surface of Rift Valley fever virus. Cell Rep. *25*, 3750–3758.e4.

Arishi, H.M., Aqeel, A.Y., and Al Hazmi, M.M. (2006). Vertical transmission of fatal Rift Valley fever in a newborn. Ann. Trop. Paediatr. *26*, 251–253.

Battles, J.K., and Dalrymple, J.M. (1988). Genetic variation among geographic isolates of Rift Valley fever virus. Am. J. Trop. Med. Hyg. *39*, 617–631.

Baudin, M., Jumaa, A.M., Jomma, H.J.E., Karsany, M.S., Bucht, G., Naslund, J., Ahlm, C., Evander, M., and Mohamed, N. (2016). Association of Rift Valley fever virus infection with miscarriage in Sudanese women: a cross-sectional study. Lancet Glob. Health *4*, e864–e871.

Besselaar-Blackburn (1992). The Synergistic Neutralization of Rift Valley Fever Virus by Monoclonal Antibodies to the Envelope Glycoproteins. Arch. Virol. *125*, 239–250.

Besselaar, T.G., and Blackburn, N.K. (1991). Topological mapping of antigenic sites on the Rift Valley fever virus envelope glycoproteins using monoclonal antibodies. Arch. Virol. *121*, 111–124.

Bett, B., Lindahl, J., Sang, R., Wainaina, M., Kairu-Wanyoike, S., Bukachi, S., Njeru, I., Karanja, J., Ontiri, E., Kariuki Njenga, M., et al. (2018). Association between Rift Valley fever virus seroprevalences in livestock and humans and their respective intra-cluster correlation coefficients, Tana River County, Kenya. Epidemiol. Infect. *5*, 1–9.

Brown, R.D., Scott, G.R., and Dalling, T. (1957). Persistence of antibodies to Rift Valley fever in man. Lancet *270*, 345.

Calarota, S.A., and Baldanti, F. (2013). Enumeration and characterization of human memory T cells by enzyme-linked immunospot assays. Clin. Dev. Immunol. *2013*, 637649.

Cdc. (2020). Rift Valley Fever (RVF) outbreak summaries. https://www.cdc.gov/vhf/rvf/outbreaks/summaries.html.

Daubney, R., Hudson, J.R., and Garnham, P.C. (1931). Enzootic hepatitis or rift valley fever. An undescribed virus disease of sheep cattle and man from east africa. J. Pathol. Bacteriol. *34*, 545–579.

Dodd, K.A., McElroy, A.K., Jones, M.E., Nichol, S.T., and Spiropoulou, C.F. (2013). Rift Valley fever virus clearance and protection from neurologic disease are dependent on CD4+ T cell and virus-specific antibody responses. J. Virol. *87*, 6161–6171.

Easterday, B.C. (1965). Rift valley fever. Adv. Vet. Sci. *10*, 65–127.

Ellgaard, L., and Helenius, A. (2003). Quality control in the endoplasmic reticulum. Nat. Rev. Mol. Cell Biol. *4*, 181–191.

Findlay, G.M. (1936). The Mechanism of Immunity in Rift Valley Fever (Wellcome Bureau of Scientific Research)), pp. 89–104.

Freiberg, A.N., Sherman, M.B., Morais, M.C., Holbrook, M.R., and Watowich, S.J. (2008). Three-dimensional organization of Rift Valley fever virus revealed by cryoelectron tomography. J. Virol. *82*, 10341–10348.

Gouglas, D., Thanh Le, T., Henderson, K., Kaloudis, A., Danielsen, T., Hammersland, N.C., Robinson, J.M., Heaton, P.M., and Røttingen, J.-A. (2018). Estimating the cost of vaccine development against epidemic infectious diseases: a cost minimisation study. Lancet Glob. Health *6*, e1386–e1396.

Gutjahr, B., Keller, M., Rissmann, M., Von Arnim, F., Jackel, S., Reiche, S., Ulrich, R., Groschup, M.H., and Eiden, M. (2020). Two monoclonal antibodies against glycoprotein Gn protect mice from Rift Valley Fever challenge by cooperative effects. PLoS Negl. Trop. Dis. *14*, e0008143.

Halldorsson, S., Behrens, A.J., Harlos, K., Huiskonen, J.T., Elliott, R.M., Crispin, M., Brennan, B., and Bowden, T.A. (2016). Structure of a phleboviral envelope glycoprotein reveals a consolidated model of membrane fusion. Proc. Natl. Acad. Sci. U S A *113*, 7154–7159.

Halldorsson, S., Li, S., Li, M., Harlos, K., Bowden, T.A., and Huiskonen, J.T. (2018). Shielding and activation of a viral membrane fusion protein. Nat. Commun. *9*, 349.

Harmon, J.R., Barbeau, D.J., Nichol, S.T., Spiropoulou, C.F., and McElroy, A.K. (2020). Rift Valley fever virus vaccination induces long-lived, antigen-specific human T cell responses. NPJ Vaccin. *5*, 17.

Huiskonen, J.T., Overby, A.K., Weber, F., and Grunewald, K. (2009). Electron cryo-microscopy and single-particle averaging of Rift Valley fever virus: evidence for GN-GC glycoprotein heterodimers. J. Virol. *83*, 3762–3769.

Ictv. (2020). International Committee on Taxonomy of Viruses (ICTV). https://talk.ictvonline.org/taxonomy/.

Jansen Van Vuren, P., Tiemessen, C.T., and Paweska, J.T. (2011). Anti-nucleocapsid protein

immune responses counteract pathogenic effects of Rift Valley fever virus infection in mice. PLoS One *6*, e25027.

Keegan, K., and Collett, M.S. (1986). Use of bacterial expression cloning to define the amino acid sequences of antigenic determinants on the G2 glycoprotein of Rift Valley fever virus. J. Virol. *58*, 263–270.

LaBeaud, D. (2010). Towards a safe, effective vaccine for Rift Valley fever virus. Future Virol. *5*, 675–678.

Lagerqvist, N., Naslund, J., Lundkvist, A., Bouloy, M., Ahlm, C., and Bucht, G. (2009). Characterisation of immune responses and protective efficacy in mice after immunisation with Rift Valley Fever virus cDNA constructs. Virol. J. *6*, 6.

Li, S., Rissanen, I., Zeltina, A., Hepojoki, J., Raghwani, J., Harlos, K., Pybus, O.G., Huiskonen, J.T., and Bowden, T.A. (2016). A Molecular-Level Account of the Antigenic Hantaviral Surface. Cell reports *15*, 959–967.

Lopez-Gil, E., Lorenzo, G., Hevia, E., Borrego, B., Eiden, M., Groschup, M., Gilbert, S.C., and Brun, A. (2013). A single immunization with MVA expressing GnGc glycoproteins promotes epitope-specific CD8+-T cell activation and protects immune-competent mice against a lethal RVFV infection. PLoS Negl. Trop. Dis. *7*, e2309.

Lopez-Gil, E., Moreno, S., Ortego, J., Borrego, B., Lorenzo, G., and Brun, A. (2020). MVA vectored vaccines encoding Rift Valley fever virus glycoproteins protect mice against lethal challenge in the absence of neutralizing antibody responses. Vaccines (Basel) *8*, 82.

McElroy, A.K., and Nichol, S.T. (2012). Rift Valley fever virus inhibits a pro-inflammatory response in experimentally infected human monocyte derived macrophages and a pro-inflammatory cytokine response may be associated with patient survival during natural infection. Virology *422*, 6–12.

Mehand, M.S., Al-Shorbaji, F., Millett, P., and Murgue, B. (2018). The WHO R&D Blueprint: 2018 review of emerging infectious diseases requiring urgent research and development efforts. Antiviral Res. *159*, 63–67.

Munyua, P., Murithi, R.M., Wainwright, S., Githinji, J., Hightower, A., Mutonga, D., Macharia, J., Ithondeka, P.M., Musaa, J., Breiman, R.F., et al. (2010). Rift Valley fever outbreak in livestock in Kenya, 2006–2007. Am. J. Trop. Med. Hyg. *83*, 58–64.

Nicholas, D.E., Jacobsen, K.H., and Waters, N.M. (2014). Risk factors associated with human Rift Valley fever infection: systematic review and meta-analysis. Trop. Med. Int. Health *19*, 1420–1429.

Niklasson, B.S., Meadors, G.F., and Peters, C.J. (1984). Active and passive immunization against Rift Valley fever virus infection in Syrian hamsters. Acta Pathol. Microbiol. Immunol. Scand. C *92*, 197–200.

Peters, C.J., Jones, D., Trotter, R., Donaldson, J., White, J., Stephen, E., and Slone, T.W., Jr. (1988). Experimental Rift Valley fever in rhesus macaques. Arch. Virol. *99*, 31–44.

Pittman, P.R., Norris, S.L., Brown, E.S., Ranadive, M.V., Schibly, B.A., Bettinger, G.E., Lokugamage, N., Korman, L., Morrill, J.C., and Peters, C.J. (2016). Rift Valley fever MP-12 vaccine Phase 2 clinical trial: safety, immunogenicity, and genetic characterization of virus isolates. Vaccine *34*, 523–530.

Rissanen, I., Stass, R., Krumm, S.A., Seow, J., Hulswit, R.J.G., Paesen, G.C., Hepojoki, J., Vapalahti, O., Lundkvist, Å., Reynard, O., et al. (2020). Molecular rationale for hantavirus neutralization by a reservoir host-derived monoclonal antibody. bioRxiv. 2020.04.17. 029876.

Rissanen, I., Stass, R., Zeltina, A., Li, S., Hepojoki, J., Harlos, K., Gilbert, R.J.C., Huiskonen, J.T., and Bowden, T.A. (2017). Structural Transitions of the Conserved and Metastable Hantaviral Glycoprotein Envelope. J. Virol. 91.

Scott, J.a.G., Bauni, E., Moisi, J.C., Ojal, J., Gatakaa, H., Nyundo, C., Molyneux, C.S., Kombe, F., Tsofa, B., Marsh, K., et al. (2012). Profile: the Kilifi Health and demographic surveillance system (KHDSS). Int. J. Epidemiol. *41*, 650–657.

Sherman, M.B., Freiberg, A.N., Holbrook, M.R., and Watowich, S.J. (2009). Single-particle cryo-electron microscopy of Rift Valley fever virus. Virology *387*, 11–15.

Smithburn, K.C., Mahaffy, A.F., Haddow, A.J., Kitchen, S.F., and Smith, J.F. (1949). Rift Valley fever; accidental infections among laboratory workers. J. Immunol. *62*, 213–227.

Vidarsson, G., Dekkers, G., and Rispens, T. (2014). IgG subclasses and allotypes: from structure to effector functions. Front. Immunol. *5*, 520.

Wang, Q., Ma, T., Wu, Y., Chen, Z., Zeng, H., Tong, Z., Gao, F., Qi, J., Zhao, Z., Chai, Y., et al. (2019). Neutralization mechanism of human monoclonal antibodies against Rift Valley fever virus. Nat. Microbiol. 1231–1241.

Weingartl, H.M., Zhang, S., Marszal, P., Mcgreevy, A., Burton, L., and Wilson, W.C. (2014). Rift Valley fever virus incorporates the 78 kDa glycoprotein into virions matured in mosquito C6/36 cells. PLoS One *9*, e87385.

Wonderlich, E.R., Caroline, A.L., Mcmillen, C.M., Walters, A.W., Reed, D.S., Barratt-Boyes, S.M., and Hartman, A.L. (2018). Peripheral blood biomarkers of disease outcome in a monkey model of Rift Valley fever encephalitis. J. Virol. *92*, e01662–17.

Wright, D., Kortekaas, J., Bowden, T.A., and Warimwe, G.M. (2019). Rift Valley fever: biology and epidemiology. J. Gen. Virol. *100*, 1187–1199.

Supplemental Information

Naturally Acquired Rift Valley

Fever Virus Neutralizing Antibodies

Predominantly Target the Gn Glycoprotein

Daniel Wright, Elizabeth R. Allen, Madeleine H.A. Clark, John N. Gitonga, Henry K. Karanja, Ruben J.G. Hulswit, Iona Taylor, Sumi Biswas, Jennifer Marshall, Damaris Mwololo, John Muriuki, Bernard Bett, Thomas A. Bowden, and George M. Warimwe
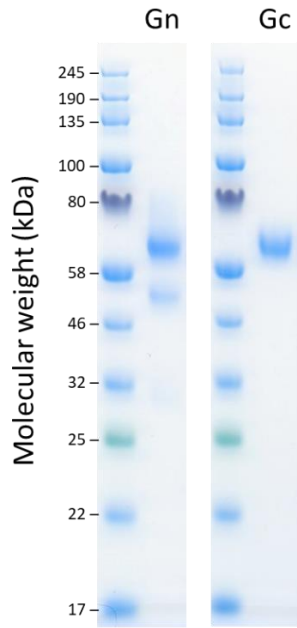
Figure S1. *SDS-PAGE of recombinant RVFV Gn (AviTagged) and Gc (SUMO-tagged), related to Figures 1, 2 and 3. Samples were loaded with reducing buffer on a NuPAGE 4-12 % Mini poly-acrylamide gel and stained with Coomassie Brilliant Blue.*
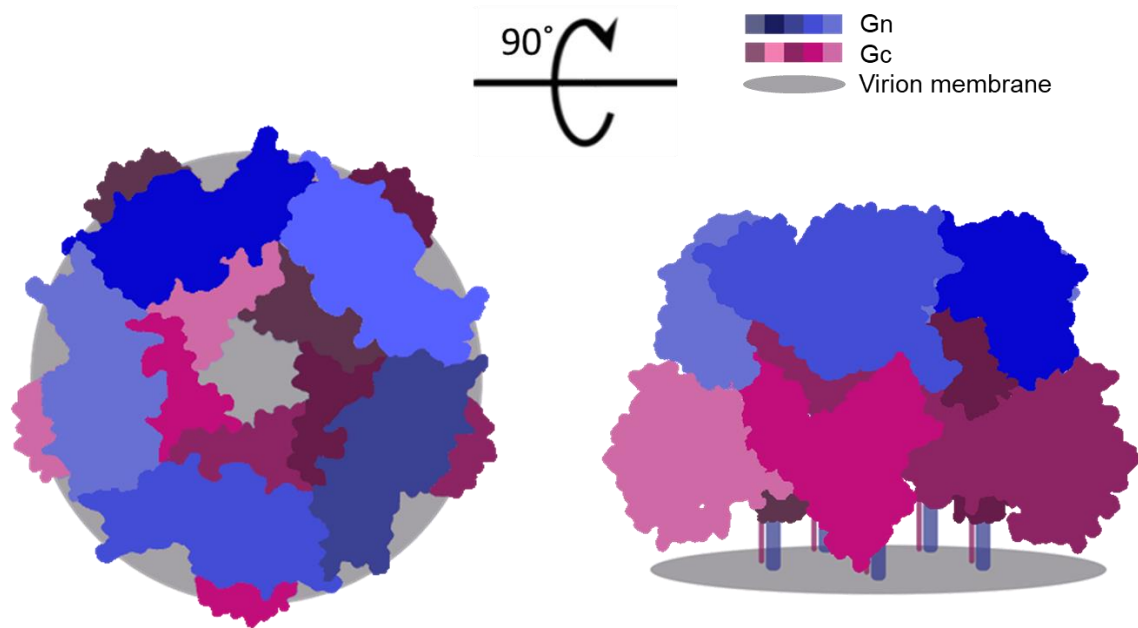
Figure S2. *Schematic representation of RVFV Gn-Gc, related to Figures 1, 2 and 3. Top (left) and side views (right) of a schematic surface representation of the pentameric assembly of envelope-displayed RVFV Gn-Gc heterodimers based upon integrative cryoEM and X-ray crystallography (PDB ID: 6F9F) (Halldorsson et al., 2018). Pentamers and hexamers of Gn-Gc heterodimers encapsulate RVFV with T=12 icosahedral symmetry. Each membrane-distally located RVFV Gn is rendered in a shade of blue and each membrane-proximally located RVFV Gc is rendered in a shade of purple. The C-terminal regions of RVFV Gn and Gc are shown as lines due to the lack of high resolution structural information and are anchored to the virion membrane (grey).*

TRANSPARENT METHODS

Study population

A cross-section of randomly selected households in Tana River County, Kenya (2013-2014) were enrolled after consenting and all human subjects within that household were sampled as part of a previous study estimating RVFV exposure (Bett et al., 2018) . For this analysis, serum samples from 50 adults ≥18 years old (n = 26 male, n = 24 female) were selected at random for antibody characterization from those identified as RVFV-exposed on the basis of seropositivity by both RVFV neutralization assay (VNT$_{50}$ >10) and a diagnostic ELISA kit (BDSL, National Institute for Communicable Diseases, Centre for Emerging and Zoonotic Diseases, Johannesburg, South Africa) (Paweska et al., 2005). A further 7 RVFV-exposed individuals from the same study were assessed in the antibody depletion assays. Serum and peripheral blood mononuclear cells (PBMCs) were available from 200 adults ≥18 years old (n = 72 male, n = 128 female) under longitudinal surveillance for malaria studies in Kilifi County in 2018. For some of these adults, serum samples were available dating back to 1998 when they were enrolled into the longitudinal cohort. Additional screening of the serum samples collected in 2013-2014 identified positive individuals not sampled in 2018. Blood samples were collected in plain vacutainers and serum harvested after centrifugation at 1,000 RCF for 5 minutes, before storage at -80°C until use. Heparinised blood was used for PBMC isolation using standard protocols (Illingworth et al., 2013) and were resuspended in FCS containing 10% DMSO prior to freezing. Vials containing ~5x10^6 PBMC in 1mL were slowly cooled to -80ºC in Mr Frosty's before being transferred to liquid nitrogen until use. Ethical approval for this study was provided by the Kenya Medical Research Institute Scientific and Ethics Review Unit (SSC 3296), and the African Medical Research Foundation's Ethics and Scientific Review Committee (approval number P65-2013).

Protein Expression

RVFV Gn: cDNA of the Gn ectodomain (UniProt accession number P21401, residues 154-560) was cloned into pHLSec mammalian expression vector, which encodes a C-terminal hexa-histidine tag (Aricescu et al., 2006). Human embryonic kidney cells (HEK293T, ATCC CRL-1573) were transiently transfected. After 4 days Gn protein was purified from clarified cell supernatant by immobilized nickel-affinity chromatography (IMAC), using 5 mL HisTrap FF crude column and AKTA FPLC system (GE Healthcare). Gn protein was further purified by size exclusion chromatography (SEC) using a Superdex 200 10/300 Increase column (GE Healthcare) into 10mM Tris-HCl, 150mM NaCl, pH 8.0. (**Fig. S1**)

RVFV Gc: cDNA of the Gc ectodomain (UniProt accession number P21401, residues 691-1139) linked to an N-terminal SUMO tag, which also encodes a hexa-histidine tag, was subcloned into the pURD expression vector to generate a stable cell line in HEK293T cells (Seiradake et al., 2015). Cells were harvested after 5 days and RVFV Gc was purified from clarified cell supernatant by IMAC. The SUMO-tag was cleaved with 3C protease (Pearsons) overnight at room temperature. Cleaved RVFV Gc was purified from the SUMO-tag by IMAC. The flowthrough containing Gc was further purified by SEC using a Superdex 200 10/300 Increase column (GE Healthcare) into 10mM Tris-HCl, 150mM NaCl, pH 8.0. (**Fig. S1**)

Standardised ELISA for detection of antigen-specific IgG

Total anti-Gn and anti-Gc IgG were measured by an indirect ELISA using a standard curve consisting of a pool of serum from individuals with high levels of RVFV neutralising antibody. 96 well NUNC flat bottom plates (ThermoFisher) were coated with 50 µl/well of Gn or Gc at a concentration of 1 µg/mL in phosphate buffered saline (PBS, Sigma) and incubated overnight at room temperature (RT). Plates were washed 6x with PBS containing 0.05% Tween20 (PBS/T) followed by blocking with 100 µl/well of 1% Blocker™ Casein in PBS (ThermoFisher) for 1 hour at RT. Plates were then tapped dry and test sera was diluted in casein, 50 µl/well was added to duplicate wells. Wells containing non-immune sera and containing casein alone were included on each plate as negative controls. A two-fold dilution series of the positive standard pool, from 1:100 to 1:51,200 in duplicate, was added to give 10 standard points. The 1:100 standard was assigned 10 arbitrary units (AU), with each subsequent point assigned half the amount. An internal control of the positive standard pool diluted at 1:800 was also included on each plate to assess plate-to-plate variation. Plates were incubated for 2h at RT. Plates were washed as before and 50 µl/well of secondary antibody (goat anti-human whole IgG conjugated to HRP, Insight

Biotechnology) was diluted 1:1,000 in casein and added to the plate for 1h at RT. Plates were washed a final time and developed by adding 50 µl/well of TMB developer (Abcam). After 8 minutes incubating in the dark at RT, 50 µl TMB stop solution (Abcam) was added. The optical density (OD) was read at 450 nm using a Varioskan flash reader. OD values were fitted to a 4-Parameter logistic model (Gen5 v3.09, BioTek) standard curve. Test sera arbitrary units (AU) were calculated from their OD values using the parameters estimated from the standard curve.

IgG avidity ELISAs

Total IgG avidity was determined by sodium thiocyanate (NaSCN) displacement, as described previously (Biswas et al., 2014). Briefly, sera were individually diluted in casein to normalise titers, according to their total IgG ELISA AU. Plate coating, blocking and development were performed the same as their respective total IgG ELISAs.

IgG Subclass ELISAs

IgG subclass ELISAs were performed as per the total IgG ELISAs with the following exceptions: Secondary antibodies (biotin conjugated mouse anti-human IgG1, IgG2, IgG3 or IgG4 [Bio-Rad]) were incubated for 1h. After washing, 50 µL/well of eXtravidin-ALP (Sigma), diluted 1:5,000 in casein was added for 1h. Plates were washed and then developed by adding 50 µl/well of 4-nitrophenyl phosphate in diethanolamine buffer (Pierce). OD was read at 405 nm.

Virus Neutralization assays (VNT and FRNT)

VNT: The dilution required to reduce neutralization by 50% (VNT_{50}) was calculated, as described previously (Lopez-Gil et al., 2013). Briefly, serum pools were diluted in DMEM containing 10% FCS across a 96-well plate before addition of 100 $TCID_{50}$ of RVFV MP-12 strain. Sera and virus were incubated at 37 °C for 1h in 200 µl before being added to a 96 well tissue culture (TC) plate containing a confluent monolayer of VERO cells. Plates were incubated at 37 °C for 72h before cells were fixed in PBS containing 10% formaldehyde for 1h and stained with PBS containing 1% crystal violet (Sigma) for 10 minutes. Plates were washed with water and left to dry before being scored by eye. Focus reduction neutralizing test (FRNT): This was carried out as previously described (Barsosio et al., 2019) with some alterations. Briefly, serum was diluted in 2-fold steps in triplicate from a starting dilution of 1:20. Approximately 100 focus-forming units of RVFV (MP-12 strain) was added to each well and incubated for 1h at 37 °C before transferring mixture to 96-well Tissue Culture plate containing Vero E6 monolayers at 90% confluency. After 2h at 37 °C, virus/serum was removed and replaced with media. Plates were incubated a further 48h at 37 °C. Virus foci were detected by adding 1:1000 dilution of Anti-Gn 4D4 mouse mAb (bei resources, Cat. No. NR-43190) followed by 1:1000 dilution of horseradish peroxidase (HRP)-conjugated goat anti-mouse IgG antibody (Abcam, Cat. No. ab6789). After addition of 3,3'-diaminobenzidine (Sigma) substrate for 10 minutes at room temperature, the plates were washed a final time and air dried. Foci were counted using an AID ELISpot reader. Serum dilution required to reduce virus foci by 50% compared to virus-only control wells (6 replicates) was calculated from a 4-parameter standard curve using GraphPad Prism version 8 (GraphPad Software Inc., California, USA).

Gn and Gc specific antibody depletion

In order to deplete anti-Gc and/or anti-Gn IgG, 96-well NUNC ELISA plates were coated with 5 µg/mL of recombinant Gn or Gc or carbonate-bicarbonate buffer alone. Plates were incubated overnight. After washing with PBS/T as previously described, plates were blocked with 200 µL/well of 1% casein in PBS (Sigma) for 2h. Neat pooled human sera was diluted 1:50 in DMEM containing 2% L-glutamine and 1% penicillin/streptomycin with subsequent 1:2 titrations up to 1:102400. Diluted sera was added to each antigen-coated plate (including the blocked but uncoated control plate) and incubated on a plate rocker at 10 RPM for 4h at room temperature. Serum was then removed and the depletion step repeated once more on additional coated and blocked plates. For the dual Gn/Gc depletion, serum was depleted twice on Gn-coated plates and twice on Gc-coated plates. Reduction of antigen-specific antibodies after final depletion was confirmed by ELISA. Serum was diluted 1:2 with Casein and total IgG ELISA was carried out as described. The endpoint titer is defined as the interpolated dilution (OD at 450nm versus dilution of serum) at which the OD of the sample is 0.15. The remaining serum was added to the VNT or FRNT

plate to determine nAb titer, as previously described, with final serum concentrations ranging from 1:200-1:102,400.

Ex-vivo IFNγ ELISpot

264 15mer peptides overlapping by 11 amino acids, covering the Gn-Gc polyprotein (Genbank accession number DQ380208, residues 132-1197) were synthesised (Mimotopes). Peptides were split into 5 pools of 52/53 peptides each at 1.25 µg/mL final concentration. ELISpots were carried out as previously described (Kimani et al., 2014). Responses from unstimulated wells were subtracted before quantifying the response to the 5 pools and summing them. Positive control wells were stimulated with SEB at 0.02 µg/mL.

Statistical analysis

Statistical analysis was carried out using GraphPad Prism version 8 (GraphPad Software Inc., California, USA). All analyses of correlations were performed using non-parametric Spearman's correlation tests using a two-sided p value < 0.05 as the cut-off for statistical significance. Comparisons between two groups were analysed using Kruskal-Wallis test or unpaired T-test.

SUPPLEMENTAL REFERENCES

Aricescu, A. R., Lu, W. & Jones, E. Y. 2006. A time-and cost-efficient system for high-level protein production in mammalian cells. Acta Crystallogr D Biol Crystallogr,62, 1243-50.

Barsosio, H. C., Gitonga, J. N., Karanja, H. K., Nyamwaya, D. K., Omuoyo, D. O., Kamau, E., Hamaluba, M. M., Nyiro, J. U., Kitsao, B. S., Nyaguara, A., et al. 2019. Congenital microcephaly unrelated to flavivirus exposure in coastal Kenya. Wellcome Open Res,4, 179.

Biswas, S., Choudhary, P., Elias, S. C., Miura, K., Milne, K. H., De Cassan, S. C., Collins, K. A., Halstead, F. D., Bliss, C. M., Ewer, K. J., et al. 2014. Assessment of humoral immune responses to blood-stage malaria antigens following ChAd63-MVA immunization, controlled human malaria infection and natural exposure. PLoS One,9, e107903.

Illingworth, J., Butler, N. S., Roetynck, S., Mwacharo, J., Pierce, S. K., Bejon, P., Crompton, P. D., Marsh, K. & Ndungu, F. M. 2013. Chronic exposure to Plasmodium falciparum is associated with phenotypic evidence of B and T cell exhaustion. Journal of immunology (Baltimore, Md. : 1950),190, 1038-1047.

Kimani, D., Jagne, Y. J., Cox, M., Kimani, E., Bliss, C. M., Gitau, E., Ogwang, C., Afolabi, M. O., Bowyer, G., Collins, K. A., et al. 2014. Translating the immunogenicity of prime-boost immunization with ChAd63 and MVA ME-TRAP from malaria naive to malaria-endemic populations. Mol Ther,22, 1992-2003.

Paweska, J. T., Mortimer, E., Leman, P. A. & Swanepoel, R. 2005. An inhibition enzyme-linked immunosorbent assay for the detection of antibody to Rift Valley fever virus in humans, domestic and wild ruminants. Journal of Virological Methods,127, 10-18.

Seiradake, E., Zhao, Y., Lu, W., Aricescu, A. R. & Jones, E. Y. 2015. Production of cell surface and secreted glycoproteins in mammalian cells. Methods Mol Biol,1261, 115-27